Detection of Possible Anomalies in the Transit Lightcurve of Exoplanet TrES-1b Using a Distributed Observer Network

Author: Ron Bissinger[(1)]
Contributors: Dr. Greg Laughlin[(2)], Dr. Tim Castellano[(3)], Bruce Gary[(4)], Joe Garlitz[(5)], Tonny Vanmunster[(6)], Pertti Pääkkönen[(7)], Tommi Itkonen[(7)], Kent Richardson[(8)], Jon Holtzman[(9)]

ABSTRACT

Through a collaboration by amateur and professional astronomers functioning as a distributed observers network, apparent anomalies have been identified in the transit lightcurves of exoplanet TrES-1b made by different observers at multiple times. A detailed visual analysis of the lightcurves reveal brightenings of 3 to 5 mmag before ingress and after egress as well as short term fluctuations of < 3mmag for durations of approximately 10 minutes. The anomalies appear to be symmetrical around the transit midpoint. A rigorous bootstrap Monte Carlo analysis indicates a high probability that the lightcurve brightenings before ingress and after egress are statistically significant.

1. Introduction

1.1 Exoplanet Searches and Detection

Detection of exoplanets has been done using either radial velocity measurements or the slight drop in light as an exoplanet crosses, or transits, its parent star as viewed from earth. The first method requires the use of large professional observatories to detect the slight wobble in a star caused by an orbiting exoplanet. The second method can employ large as well as small telescopes to detect the small decreases in light caused by an exoplanet transit.

While the number of confirmed exoplanets continue to grow well past 100, only five are currently known to transit their parent stars as viewed from earth: HD209458b, OGLE-TR56b, OGLE-TR113b, OGLE-132b, and TrES –1b. The transit of HD209458b was confirmed after its initial discovery using radial velocity measurements. The remaining four exoplanets were discovered using the transit method.

Numerous organized efforts are underway to discover more exoplanets using the transit method, including STARE, PSST, TrES, SLEUTH, Transitsearch, and many others. Most of the searches conduct wide field surveys using instruments with apertures smaller than 20cm. Some searches, including the Transitsearch effort, use a more targeted approach and monitor candidates with high metallicities, for example.

Exoplanet searches are not limited to ground-based observations. Both the European-sponsored COROT mission, slated for launch in 2006, and the NASA Kepler mission scheduled for a 2007 launch will seek the presence of exoplanets using the transit method. Hundreds of additional exoplanets are expected to be identified by these missions, including some that may be close to earth in size.

1.2. Amateur/Professional Collaborations and the Distributed Observing Network

Computerized 20cm to 35cm telescopes and highly sensitive cooled CCD cameras have been widely adopted by serious amateur astronomers and universities due to their relative affordability and high quality. Dedicated users of these systems have been able to perform precise

measurements of stellar flux (photometry) and position (astrometry) which a decade ago were the sole province of large professional observatories.

Observing time at large professional observatories comes at a premium and is often rationed among professional astronomers. Such large observatories usually cannot afford to conduct long term monitoring of objects due to numerous competing priorities. The serious amateur astronomer on the other hand can spend the time on long term observing campaigns of specific objects identified by professional astronomers. Amateur astronomers around the world are now coordinated over the web as a distributed observer network providing continuous coverage across many time zones and around adverse local weather conditions.

Not only is the geographic coverage provided by the distributed observer network valuable, but the data gathered from many observers can be combined to obtain levels of precision that cannot often be attained by any single observer. By "stacking" the individual data sets noise is reduced inversely proportional to the square root of the number of data sets used, a technique that increases the ratio of useful signal to noise. Large professional observatories often cannot afford to generate multiple observation data sets of single objects whereas a distributed network of amateur and university observers can.

As an example of the distributed observer network and collaboration between amateur and professional astronomers, the Transitsearch project[11] has recently partnered with the American Association of Variable Star Observers (AAVSO)[12] to conduct observing campaigns on specific targets of interest identified by professional astronomers. Participants in these campaigns are amateur astronomers using CCD cameras on telescopes commonly having apertures ranging from 20cm to 51cm as well as university observatories having even larger instruments. Most of the participants have demonstrated ability to obtain precision photometry (10 mmag or better) on stars brighter than about 12th magnitude and continue to hone their skills observing the known transiting exoplanets.

As new exoplanets are discovered using ground- and space-based telescopes a distributed observer network can do useful science by providing additional multiple high quality observations over long time periods that large professional observatories cannot afford to make. It is almost certain that some exoplanets will have ring systems or other physical attributes that can be characterized by multiple observations over time.

1.3 TrES-1b and the Distributed Observer Network

The recent discovery by Alonso et al [12] of the transiting exoplanet TrES-1b prompted many Transitsearch and AAVSO participants to capture its transit lightcurve. The parent star of TrES-1b exhibits a visual magnitude of 11.7 and is well positioned for observing in mid to late summer in the northern hemisphere. Starting in early September 2004 Transitsearch participants began posting their transit lightcurves on the group's website, the first of which came from Tonny Vanmunster (Belgium). Additional lightcurves were posted throughout September by Samo Smrke and Nicolaj Stritof (Slovenia), Ondrej Pejcha (Czech Republic), Pertti Pääkkönen and Tommi Itkonen (Finland), Robin Leadbeater (UK), Bruce Gary (Arizona, USA), Joe Garlitz (Oregon, USA) and the author. In late September Gary and Garlitz observed that there were apparent brightenings and dimmings near the ingress and egress of the lightcurves, something that was not expected based on lightcurves obtained from other transiting exoplanets.

In subsequent postings in the Transitsearch user group various possible explanations were offered for the TrES-1b anomalies including satellites, a ring system, and dust clouds. Before any such explanation can be considered, it is first necessary to test the data to confirm the likelihood that

the apparent anomalies are actually present in the data and are not artifacts or otherwise explainable.

2. Observations and Data Precision

2.1 Database Creation

The author took up the suggestion of Dr. Greg Laughlin and others to construct a composite TrES-1b lightcurve of all available data to further examine whether anomalies were present. An Excel database was built consisting of observations cited in the Alonso et al discovery paper as well as observations from Vanmunster, Pääkkönen and Itkonen, Kent Richardson, Jon Holtzman, and the author. A total of 34 separate observations were included in the database, totaling over 4400 datapoints. More data has recently been received by the author but could not be included in the current analysis.

Table 1 shows the observations included in the database along with the predicted transit midpoint time for the observations, the aperture of the instrument used, filter and CCD camera details and the time interval of the data. Note that the time interval does not necessarily correlate to the individual exposures used during photometry as many of the observers binned their data before submission. Table 1 also specifies the portion of the TrES-1b transit lightcurve that was captured.

2.2 Observers and Equipment

The apertures used in the transit photometry ranged from 10cm to 120cm, and time intervals of the data were as short as 30 seconds and as long as 8.7 minutes. The first data were taken on May 9, 2004 and the last on October 11, 2004. Few of the observations were done at the same time by different observers. Specifications of all of the CCD cameras used are not thoroughly known at this time but are believed to cover a wide swath of equipment, including SBIG ST-7XME, SBIG ST-8XME, SBIG ST-10XME, SBIG ST-1001E cameras. The telescopes were on mounts from various manufacturers including Celestron, Meade and AstroPhysics. European observer locations included Finland, the UK, Czech Republic, Slovenia, as well as Arizona, Oregon, and California in the United States.

2.3 Data Quality and Sources of Errors

There was little consistency in the methodology used to reduce the raw CCD images and generate photometric data. It is known that at least three commercially available photometry software packages were utilized: AIP4Win, CCDSoft, and Mira AP. Different comparison stars were undoubtedly used in the photometry. While a variety of filters were used by observers, Alonso et al reported no dependency upon wavelength for the TrES-1b lightcurve, so filtration would initially be expected to have little significant effect on the lightcurves presented herein.

Another significant variable is the airmass through which the observations were made. The airmass likely ranged from low to high. Some of the early 2004 observations were probably made through high airmass, particularly the ingress portions. Observations made from the western United States in September of 2004 often were made through increasing airmass, particularly the egress portions.

There may exist an apparent asymmetry in the quality of the data because more ingress portions of the transit may have been observed through lower airmass than egress portions. This is particularly the case with the September 2004 observations from the western United States. As a

result, resolution in the composite ingress lightcurves may be higher than in the composite egress lightcurves.

Given the great differences in equipment, software and technique, one might conclude that any attempt to compare the individual datasets would be futile. However, most of the observers have learned to use their specific equipment and software as an integrated system to obtain precise, reproducible high quality photometric data before they began observing TrES-1b. Many had perfected their photometric skills on the transiting exoplanet HD209458b or on variable stars as part of other AAVSO campaigns.

2.4 Error Estimates

Most of the datasets reported errors calculated directly by the photometry software. The individual datasets used in the analyses were of high quality with errors consistently < 5mmag. When data sets are combined or stacked, the error can be further reduced inversely proportional to the square root of the number of stacked observations. Note that precisions of 1or 2 mmag from ground-based observatories is at or near the theoretical limits imposed by atmospheric seeing.

An example of the photometric precision often obtained in the TrES-1b observations is shown in Figure 1. Using a 35cm telescope, the author made six baseline photometry runs of TrES-1b on evenings when transits were not predicted to occur. The same comparison star and software was used for the photometry. All observations were made through airmass < 2. These runs were normalized and folded around the fractional time of day for easy comparison. Error limits of +/- 1 sigma are shown, based on a standard deviation calculated using a rolling boxcar of 5 datapoints. As can be seen, errors of < 5 mmag are possible with good equipment and technique, particularly when observations are stacked. Many other observers, including those contributing to this analysis, routinely do similar high quality photometry.

2.5 Varying Usefulness of Datasets

It should be noted that upon reviewing the individual datasets it became clear that the most useful data came from telescopes with apertures exceeding 30cm. The 10cm lenses used by the widefield searches of STARE, etc. are useful for detecting transits by their classic signatures but are of limited value in resolving lightcurve anomalies < 10 mmag. The long time intervals of the widefield data, over 8 minutes, also limit the data's usefulness for resolving short time frame anomalies. Telescopes exceeding 30cm also used CCD cameras with significant well depths, allowing fine flux level resolutions.

3. Normalization of Datasets

Due to the different equipment, comparison stars, filtration, airmass and other factors, the reference magnitudes in the submitted datasets needed to be normalized. Fortunately the data referred to in the Alonso et al paper was already normalized to a flux baseline of 1.0. The rest of the datasets were therefore normalized to an arbitrary magnitude baseline of 1.0 for easy visual comparison and analysis.

Many datasets shown in Table 1 only included part of the transit lightcurve. Pre-ingress portions of the lightcurve if available were used to normalize the magnitudes employing a simple least mean squares fit. The same process was employed on the post-egress portions if only the egress was observed. Where a complete lightcurve was provided the pre-ingress portion was used for normalization.

4. Visual Presentations of Anomalies in the TrES-1b Lightcurves

4.1 Replication and Symmetry of Anomalies

Initial suggestions of possible anomalies in the TrES-1b lightcurve arose from simple visual inspections of several observations. Figure 2 shows a composite curve of the full transit. There are several anomalies apparent, particularly the brightenings preceding ingress and following egress. Several features also appear to be symmetrical around the transit midpoint.

It is useful to examine more closely the datasets plotted in Figure 2 from single as well as multiple observers. Figure 3 shows the egress portion of the composite lightcurve generated by the author, and Figure 4 is the ingress portion of the same lightcurve from the author reversed for easy comparison against the egress. These curves are composites of observations taken on four separate transits. Using a rolling 12 point trend line, it is possible to visually match certain features in the ingress portion to certain features in the egress, illustrating symmetry of these apparent features around the transit midpoint. Brightenings of approximately 5 mmag are centered around 90 minutes on each side of the transit midpoint, and a dimming with a small central peak is seen around 140 minutes on each side of the transit midpoint. Although not conclusive, it also appears the features in the egress may be occurring around 10 minutes later than shown in the ingress.

Similar features and symmetry are observed in the data from the 120cm Fred L. Whipple Observatory (FLWO) taken of different transits than those shown in Figures 3 and 4. Figures 5 and 6 show charts plotting only the FLWO composite data of two transits. Again, using a rolling 12 point trendline, brightenings are seen around 80 minutes of the transit midpoint, and dimmings around 120 minutes. Although the timings of the features do not match exactly with those in the Figure 3 and 4 data from the author, they are symmetrical around the transit midpoint, and the dimming in the egress around 125 minutes appears about 10 minutes shifted from its ingress counterpart.

4.2 Short Time Frame Anomalies

Figure 7 is a high time resolution view of the ingress data from the author's 35cm telescope. Several features varying over periods of minutes and by < 3 mmag are obvious in the rolling 12 point trendline as identified in the circled areas. Applying an identical rolling 12 point trendline to non-transit baseline data made by the author yielded no similar features. The author used high cadence 30 second exposures to generate the Figure 7 data, a technique that improves the time resolution of the apparent features.

It is highly improbable that the same features seen in Figure 7 from the author's data would be seen in data from other observers if caused by noise or some random effects.

But as shown in the next three figures, the same features are clearly replicated in other observers' data of transits at different times. Figure 8 shows the ingress from Gary's 35cm data, Figure 9 from Vanmunster's 35cm data, and Figure 10 from the FLWO 120cm data. The similarity in the features, particularly in Figures 7 and 8, is readily apparent.

The common features in the lightcurves are also seen in the egress portions from different observers. Figures 11, 12, 13 and 14 show the egress data from the author, the FLWO, Vanmunster, and Gary, respectively.

4.3 Characterization of Anomalies

The features seen over long and short time frames can be visually characterized as follows:

1. Assuming a transit duration of approximately 140 minutes, an extended period of 3 – 5 mmag brightening occurs approximately 40 minutes before ingress and after egress.

2. For approximately 200 minutes before ingress and at least 130 minutes after egress there are fluctuations that last only ~10 minutes and vary by < 3 mmag. Such short term fluctuations may extend further after egress but sufficient data was not available to make that determination.

3. Both the long term and short term features are replicated in observations from multiple observers at different times with different equipment.

4. Short term fluctuations appear to decrease in intensity with time from the transit midpoint, both before ingress and after egress.

5. Monte Carlo Statistical Analysis of Anomalies

5.1 Statistical Analysis Approach

While the visual appearance of anomalies in the TrES-1b lightcurve data may seem compelling evidence of their existence, more rigorous testing was deemed necessary to determine the probability that the anomalies are statistically significant.

There are numerous known and unknown sources of errors and variability even in well-controlled photometry and particularly so when using multiple datasets from multiple observers. There can be no assurance that the data exhibits a normal Gaussian distribution and therefore application of simple statistical measures can be misleading.

At the suggestion of Dr. Greg Laughlin a bootstrap Monte Carlo simulation was applied to the data. Given a suitably large sample size, the bootstrap method essentially redistributes the existing data randomly, generating a synthetic data set. If done numerous times the procedure allows uncertainties in the data to be quantified without any assumption of a Gaussian distribution.

5.2 Null Hypothesis

To test the null hypothesis that the observed features are statistically significant, an empirical curve was employed to do a best fit on the features in the ingress and egress data. The amplitude of the features appears to decline as a function of time from the predicted transit midpoint, resembling a damped oscillation. The following equation was derived from the motion equation for a damped oscillator and used as a model for curve fitting the ingress portion of the transit:

$$m = 0.1\cos(0.071t - 0.6)e^{(-0.032t)} + 1 \qquad (1)$$

where m is the change in magnitude and t is the time from transit midpoint in minutes.

Figure 15 shows the curve fit along with a rolling 25 point trend line for comparison.

Because features in the egress lightcurve portion appear shifted from their counterparts in the ingress, the phasing in Equation 1 was adjusted for the egress curvefit as shown in Equation 2 below:

$$m = 0.1\cos(0.071t + 0.5)e^{(-0.040t)} + 1 \qquad (2)$$

A slight adjustment in the damping term from 0.032 to 0.040 was also made, reflecting the higher airmass through which the egress observations were made and the resulting faster attenuation of fluctuations in the lightcurve.

5.3 Monte Carlo Testing Methodology

A simple way to use the Excel lightcurve database was sought to perform Monte Carlo simulations. While Excel is not commonly associated with robust scientific analysis there are numerous add-in packages available that significantly enhance the spreadsheet's capabilities. An add-in package from Decisioneering of Denver, CO called Crystal Ball was used to perform the bootstrapped Monte Carlo simulations.

All bootstrap runs were made using 2,000 trials. Runs were made on the observation data sets, then on the data after the curve fit models were applied for both the ingress and egress lightcurve portions. The datasets from the author, Gary, the FLWO and Vanmunster were used as they exhibited the finer short time frame features. For ingress the datasets of the author and a composite curve of Gary, FLWO and Vanmunster datasets were tested. For egress a composite curve of Gary, FLWO, and Vanmunster datasets and the author's, Gary, FLWO and Vanmunster datasets were also tested. The observation data set had been previously normalized to a magnitude/flux of 1.0; after the curve fits were subtracted a measure of 1.0 was added to the residuals to bring the data back to a baseline of 1.0 for easy comparison purposes.

5.4 Bootstrap Monte Carlo Results

The null hypothesis was to confirm that the visually observed features were present to a statistically significant degree. The model used would also be expected to reduce the mean of the data if the brightenings near ingress and egress were removed from the data.

A dataset from the author was run twice to verify the reproducibility of the bootstrap Monte Carlo simulation. The mean was 1.00084 for one run and 1.00085 for the second, indicating a high level of reproducibility using the same dataset.

As shown in Table 2, the means as well as the 95% and 97.5% confidence levels for the means decreased as a result of applying the model. The Crystal Ball software generates extensive reports, and as an example the graphs shown in Figures 16 and 17 show the difference in the 95.7% confidence level distribution for the mean of the author's ingress dataset before and after the model was applied. Note in Figures 16 and 17 how the 97.5% confidence level for the mean shifts lower and has a noticeably wider distribution when the model is applied.

5.5 Conclusions of Statistical Testing

Based upon the results of the bootstrap Monte Carlo testing, there is a high probability that the null hypothesis is true and that the brightenings visually observed in the TrES-1b lightcurves are statistically significant.

6. Conclusions

Similar features in the TrES-1b transit lightcurves are found by visual inspection in the data from different observers at multiple times, and are reproducible by high quality photometry. Not only are the more obvious brightenings around ingress and egress present in multiple observations, but the complex, short time frame fluctuation patterns are reproduced as well. Because such patterns are seen using different instruments at different times they are unlikely to be caused by random noise.

The visual findings are further supported by a bootstrap Monte Carlo testing indicating a high probability that the major brightenings seen in the transit lightcurves are statistically significant.

The combined visual and statistical analyses support a conclusion that there is a significant likelihood that anomalies are being detected in the TrES-1b transit lightcurve.

7. Possible Causes and Implications of Anomalies in the TrES-1b Transit Lightcurves

7.1 Possible Causes of Anomalies

If it is assumed that the apparent anomalies are present in the TrES-1b lightcurves then there exists several possible causes. Ground-based observations of the TrES-1b transits measure light from the exoplanet's parent star that passes through the following light path components:

a. the immediate environment surrounding the exoplanet;
b. the environment surrounding the parent star;
c. interstellar space between the TrES-1b parent star and earth;
d. earth's atmosphere;
e. optical paths of the telescopes and CCD cameras.

Anomalies in the transit lightcurves can theoretically be created anywhere along this light path.

Multiple observers detecting the same apparent anomalies in the TrES-1b transit lightcurve would generally eliminate the last component of the light path described above. Existing observations of other transiting exoplanets such as HD209458b as well as numerous eclipsing binary stars do not exhibit the anomalies observed in the TrES-1b lightcurves, which tend to eliminate the last two light path components.

The immediate environments surrounding TrES-1b and its parent star, and the interstellar space between the exoplanet and earth, therefore remain as components of the light path that could be the source of the apparent anomalies in the TrES-1b lightcurves.

7.2 Implications of Possible Anomalies

A lightcurve created by the transit of an exoplanet without a significant atmosphere or ring system has been modeled extensively in the literature and has been confirmed by ground-based and Hubble space telescope transit observations of exoplanet HD209458b. Such transits are characterized by smooth lightcurves before and after egress, flat transit floors, and sharp shoulders at ingress and egress.

An exoplanet transit lightcurve deviating from the above model may be indicative of material either surrounding the exoplanet or its parent star. It must be emphasized that the anomalies

observed in the TrES-1b lightcurves require further confirmation and analyses before it can be concluded that either the exoplanet or its parent star have surrounding material or structure.

Several hypotheses have been offered for the anomalies, but note that none clearly explain the observations at this point.

7.3 Satellites

One of the earliest suggestions was that there might be a satellite affecting the transit lightcurve. That hypothesis is not likely because a) the lightcurve anomalies appear symmetrical around the transit midpoint, and b) current theories hold that any such satellite would be tidally locked between the planet and the parent star, precluding any significant effect on the transit light flux.

7.4 Rings

Given that all of the giant planets in our solar system have rings, exoplanets with ring systems are expected to be found. The short time frame fluctuations observed in the TrES-1b transit lightcurve resemble extinctions that could be caused by striations in a ring system, for example.

Barnes and Fortney [13] have modeled transit lightcurves for a variety of ring geometries. The observed anomalies in the TrES-1b lightcurve resemble some of their models in shape, but are not a fit because observed magnitude fluctuations between 5 and 10 mmag are significantly greater than predicted [14]. Furthermore, current models of ring systems indicate that rings should reside in the orbital plane of a close-in planet like TrES-1b and not appear obliquely as viewed from earth. If the rings were aligned in the orbital plane there would be little possibility of lightcurve brightening by forward light scattering from ring particles. Rings of close-in planets like TrES-1b should also degenerate due to pressure from solar particles (Poynting-Robertson effect) unless renewed by some mechanism.

7.5 Dust Taurus Surrounding Planet

A ring of dust orbiting the planet would be manifested by an increase in the apparent planet diameter as measured by the transit depth. A more thorough examination of the transit depths and any anomalies of the transit floor might be useful to test this hypothesis.

7.6 Activity of Parent Star

Another possibility is an active region of the parent star that rotates into view at the same time as the transit occurs, indicating the planet's orbital period and the rotation period of the parent star are the same. Such an active region would also need to be very large to cause the observed brightenings under this scenario.

7.7 Exozodiacal Clouds

Just as Vega is surrounded by a cloud of dust, it is possible that the parent star of TrES-1b is also surrounded by an exozodiacal cloud. The effects on a transit lightcurve observed through an exozodiacal cloud have not been determined, and the appearance of diffraction or other effects in the lightcurve cannot be ascertained at this point.

7.8 Apparent Anomalies are Artifacts

Lastly, despite the strong indications for their presence, it is possible that the observed lightcurve anomalies are not real or are artifacts unrelated to any physical environment surrounding TrES-1b or its parent star.

8. Recommendations

8.1 Additional Observations

The value of observations made by the distributed observer network post-discovery has been validated by the data gathered on TrES-1b. The distributed network of amateur and university observers should be further mobilized to obtain additional high quality, high cadence photometry of TrES-1b transits.

8.2 Transitsearch/AAVSO Campaign

The next observing season for the TrES-1b transits will be the summer of 2005. An observing campaign for TrES-1b should be announced in the spring of 2005 to allow participants time to build baseline lightcurves.

8.3 Additional Analysis of Transit Lightcurve Floor

The current analysis did not include any work on the transit lightcurve floors which may contain additional features similar to those seen around ingress and egress. Such work should be completed.

8.4 Involvement of Major Ground/Space Based Observatory

While additional data from small observatories will be useful, high precision/high cadence photometry obtained by high altitude observatories using a variety of filters, including polarizing filters, would be of great value confirming the existence and possible cause of the anomalies in the TrES-1b lightcurve. It may be worthwhile to observe a TrES-1b transit with a space-based observatory as was done by Hubble on HD209458b. The Hubble observations of HD209458b revealed information on the planet's atmosphere; similar observations of TrES-1b could be fruitful as well.

Acknowledgements

The author would like to thank Dr. Greg Laughlin for his encouragement and advice, Dr. Tim Castellano for his advice and guidance on precision photometry and exoplanet transits, and both of them for their contributions to Transitsearch and the amateur observing community. The author also wishes to thank Dr. Jason Barnes for his valuable insights and comments.

Author and Contributors

(1) Ron Bissinger, Racoon Run Observatory G61, Pleasanton, CA USA (925) 462-0355
rbissinger@aol.com
(2) Dr. Greg Laughlin, Assistant Professor of Astronomy and Astrophysics, University of California Santa Cruz, Santa Cruz, CA USA
(3) Dr. Tim Castellano, NASA Ames Research Center, Moffett Field, CA USA
(4) Bruce J. Gary, Hereford Arizona Observatory G95, Hereford, AZ USA
(5) Joe Garlitz, Elgin, OR USA
(6) Tonny Vanmunster, CBA Belgium Observatory, Landen, Belgium
(7) Pertti Pääkkönen, private observatory A83, Jakokoski, Finland
(7) Tommi Itkonen, private observatory A83, Jakokoski, Finland
(8) Kent Richardson, southern California, USA
(9) Jon Holtzman, New Mexico State University, Las Cruces, New Mexico USA

References

(10) – www.transitsearch.org
(11) – www.aavso.org
(12) - 2004 preprint of paper by Roi Alonso, Timothy M. Brown, Guillermo Torres, David W. Latham, Alessandro Sozzetti, Georgi Mandushev, Juan A. Belmonte, David Charbonneau, Hans J. Deeg, Edward W. Dunham, Francis T. O'Donovan, Robert P. Stefanik
(13) – J. Barnes, J. Fortney, pending publication, Astrophysical Journal
(14) – J. Barnes, private communication

		Observatory or Source	Predicted Transit Midpoint Date, JD UT During Observation	Aperture, cm	Filter	CCD Camera	Data Interval, min	Part of Transit Observed			Anomalies Observed			Ingress and/or Egress Detailed Analysis Complete
								Ingress	Bottom	Egress	< Ingress	Bottom	>Egress	
1	Alonso et al	STARE 2003 R	2453135.295	10	R		8.70							
2	Alonso et al	STARE 2003 R	2453138.325	10	R		8.70							
3	Alonso et al	STARE 2003 R	2453144.385	10	R		8.70							
4	Alonso et al	STARE 2003 R	2453156.505	10	R		8.70							
5	Alonso et al	STARE 2003 R	2453156.505	10	R		8.70							
6	Alonso et al	PSST 2004 R	2453171.656	10	R		8.80							
7	Alonso et al	PSST 2004 R	2453174.686	10	R		8.60							
8	Alonso et al	IAC80 2004 V	2453174.686	80	V		1.70	partial	complete		possibly	possibly		
9	Alonso et al	IAC80 2004 I	2453174.686	80	I		1.70	partial	complete		possibly	possibly		
10	Alonso et al	SBO 2004 B	2453180.746	61	B		3.70		complete	complete		possibly	YES	X
11	Alonso et al	SBO 2004 R	2453180.746	61	R		5.40		complete	complete		possibly	YES	X
12	Alonso et al	FLWO 2004 g	2453183.776	120	g		2.30	complete		complete	YES		YES	X
13	Alonso et al	FLWO 2004 z	2453183.776	120	z		2.40	complete		complete	YES		YES	X
14	Alonso et al	FLWO 2004 g	2453186.806	120	g		2.70	complete	complete	complete	YES	possibly	YES	X
15	Alonso et al	FLWO 2004 r	2453186.806	120	r		2.70	complete	complete	complete	YES	possibly	YES	X
16	Alonso et al	FLWO 2004 z	2453186.806	120	z		2.70	complete	complete	complete	YES	possibly	YES	X
17	Alonso et al	PSST 2004 R	2453189.836	10	R		8.70							
18	Alonso et al	PSST 2004 R	2453192.866	10	R		8.60							
19	Vanmunster, T	CbA Belgium	2453250.437	35		SBIG ST-7XME	2.58	complete	complete	complete	YES		YES	X
20	Paakkonen, P; Itkonen, T.	private A83 Finland	2453253.467	51	V	SBIG ST1001E	1.27	complete			YES			X
21	Vanmunster, T	CbA Belgium	2453253.467	35		SBIG ST-7XME	2.49	complete	complete	complete	YES		YES	X
22	Bissinger, R	Racoon Run Obs G61	2453268.618	35	R	SBIG ST-10XME	1.08			complete			YES	X
23	Gary, B	Hereford Arixona Obs G95	2453271.648	35	V	SBIG ST-8XME	3.30	partial	complete	complete	YES		YES	X
24	Bissinger, R	Racoon Run Obs G61	2453274.678	35	R	SBIG ST-10XME	1.00			complete			YES	X
25	Garlitz, J	private	2453274.678				0.66	partial	complete	partial	likely		likely	X
26	Bissinger, R	Racoon Run Obs G61	2453277.708	35	R	SBIG ST-10XME	1.50	partial	complete	complete	YES		YES	X
27	Bissinger, R	Racoon Run Obs G61	2453280.738	35	R	SBIG ST-10XME	1.50	partial	complete	partial	likely		YES	X
28	Garlitz, J	private	2453280.738				0.66	partial	complete	partial	likely		likely	X
29	Gary, B	Hereford Arixona Obs G95	2453280.738	35	R	SBIG ST-8XME	3.30	complete	complete		YES			X
30	Bissinger, R	Racoon Run Obs G61	2453283.768	35	V	SBIG ST-10XME	0.50	complete			YES			X
31	Bissinger, R	Racoon Run Obs G61	2453286.798	35	V	SBIG ST-10XME	0.50	complete			YES			X
32	Gary, B	Hereford Arixona Obs G95	2453286.798	35	R	SBIG ST-8XME	3.80	complete			YES			X
33	Bissinger, R	Racoon Run Obs G61	2453289.828	35	V	SBIG ST-10XME	0.50	complete			YES			X
34	Richardson, K	private	2453289.828	30	V	SBIG ST-7XME	2.29	complete						

Table 1 – Observation Database as of October 12, 2004

	Normalized	Residuals	% delta
INGRESS/BISSINGER			
Mean	1.00084	0.99980	-0.104%
Standard Deviation of Mean	0.00546	0.00544	-0.317%
Variance of Mean	0.00003	0.00003	-0.630%
Mean 95% Confid Level	1.01026	1.00083	-0.933%
Mean 97.5% Confid Level	1.01284	1.00988	-0.293%
2ND CHECK RUN:			
Mean	1.00085		
Standard Deviation of Mean	0.00546		
Variance of Mean	0.00003		
Mean 95% Confid Level	1.01025		
Mean 97.5% Confid Level	1.01282		
INGRESS/GARY, FLWO, VANMUNSTER			
Mean	1.00060	1.00011	-0.050%
Standard Deviation of Mean	0.00516	0.00523	1.502%
Variance of Mean	0.00003	0.00003	3.026%
Mean 95% Confid Level	1.00949	1.00809	-0.138%
Mean 97.5% Confid Level	1.01171	1.00977	-0.192%
EGRESS/GARY, FLWO, VANMUNSTER			
Mean	1.00037	1.00015	-0.022%
Standard Deviation of Mean	0.00343	0.00349	1.638%
Variance of Mean	0.00001	0.00001	3.271%
Mean 95% Confid Level	1.00594	1.00591	-0.003%
Mean 97.5% Confid Level	1.00784	1.00707	-0.076%
EGRESS/BISSINGER, GARY, FLWO, VANMUNSTER			
Mean	1.00092	0.99926	-0.166%
Standard Deviation of Mean	0.00656	0.00656	-0.085%
Variance of Mean	0.00004	0.00004	-0.172%
Mean 95% Confid Level	1.00973	1.00798	-0.173%
Mean 97.5% Confid Level	1.01290	1.01058	-0.230%

Table 2 – Results of Bootstrap Monte Carlo Testing

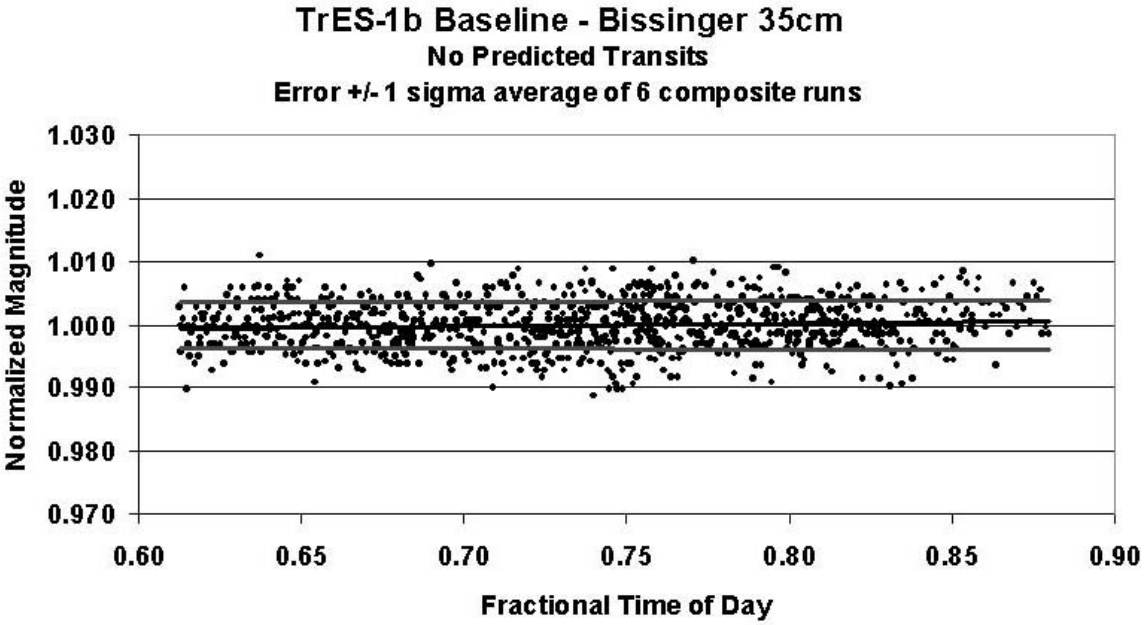

Figure 1 – Baseline Non-transiting Observations of TrES-1b

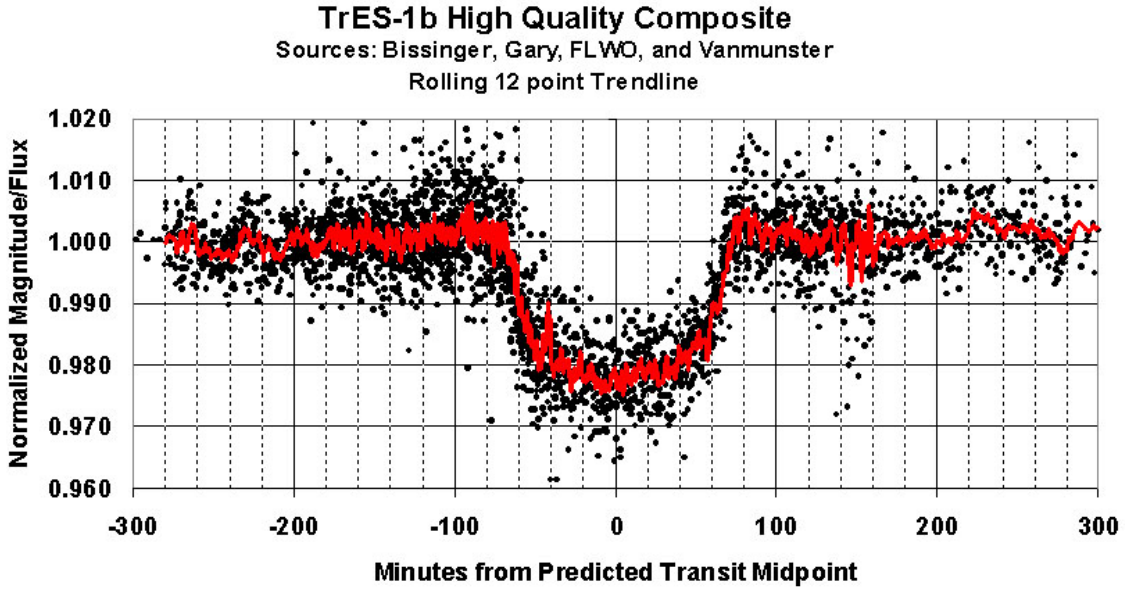

Figure 2 – Composite TrES-1b Lightcurve

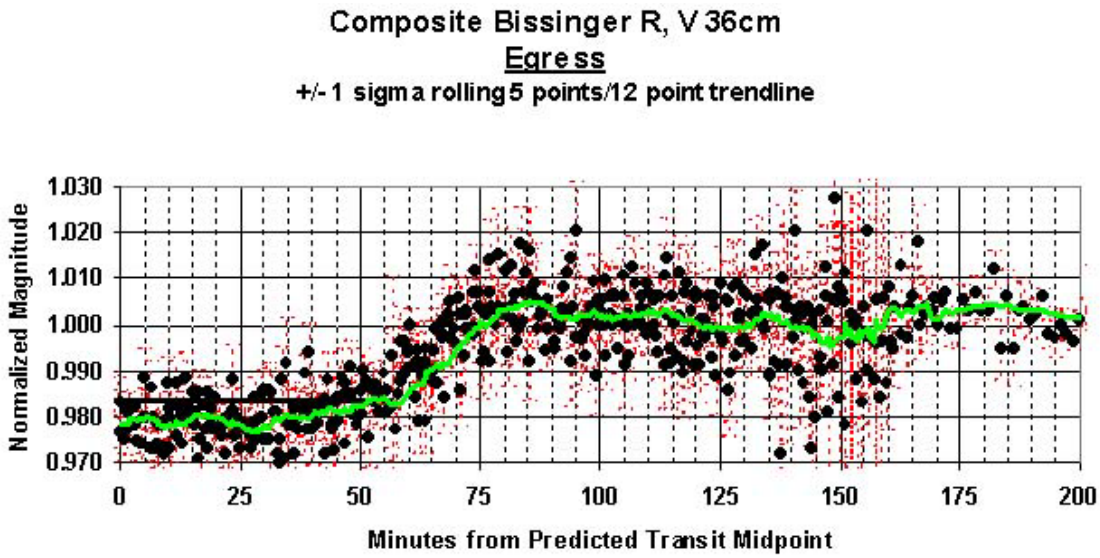

Figure 3 – Bissinger Egress

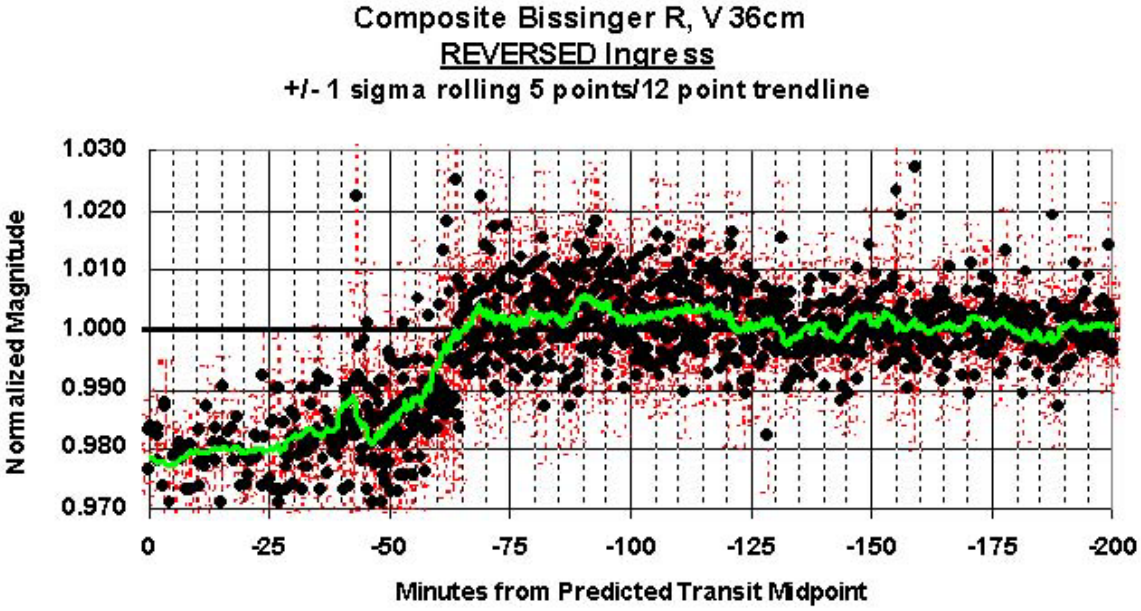

Figure 4 – Bissinger Ingress (Reversed)

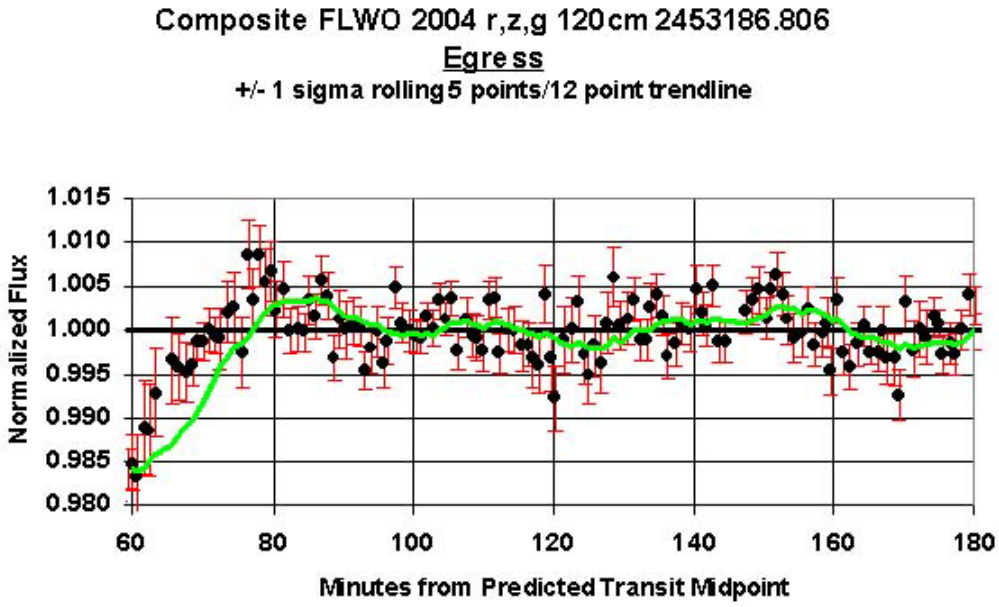

Figure 5 – FLWO Egress

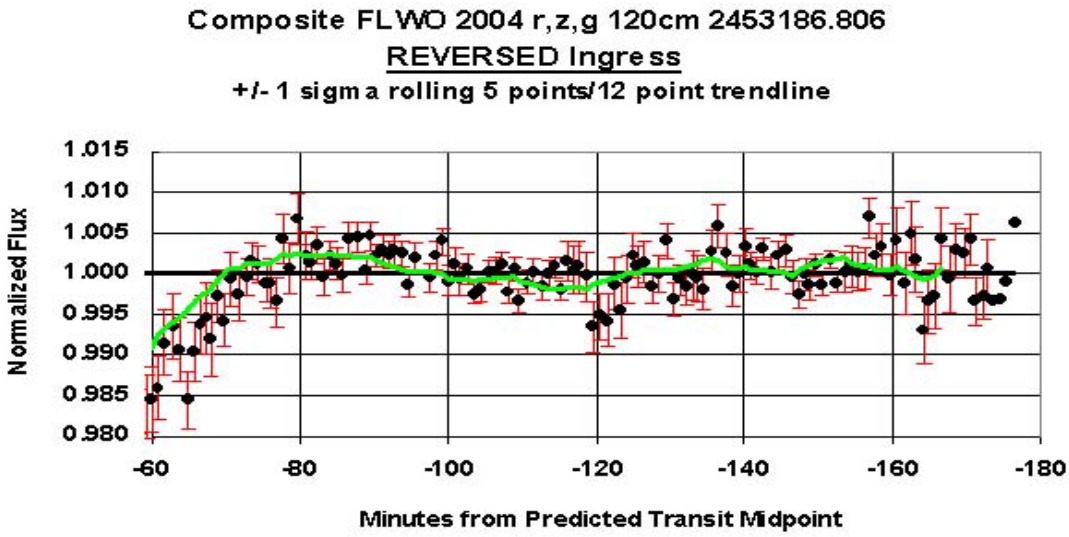

Figure 6 – FLWO Ingress (Reversed)

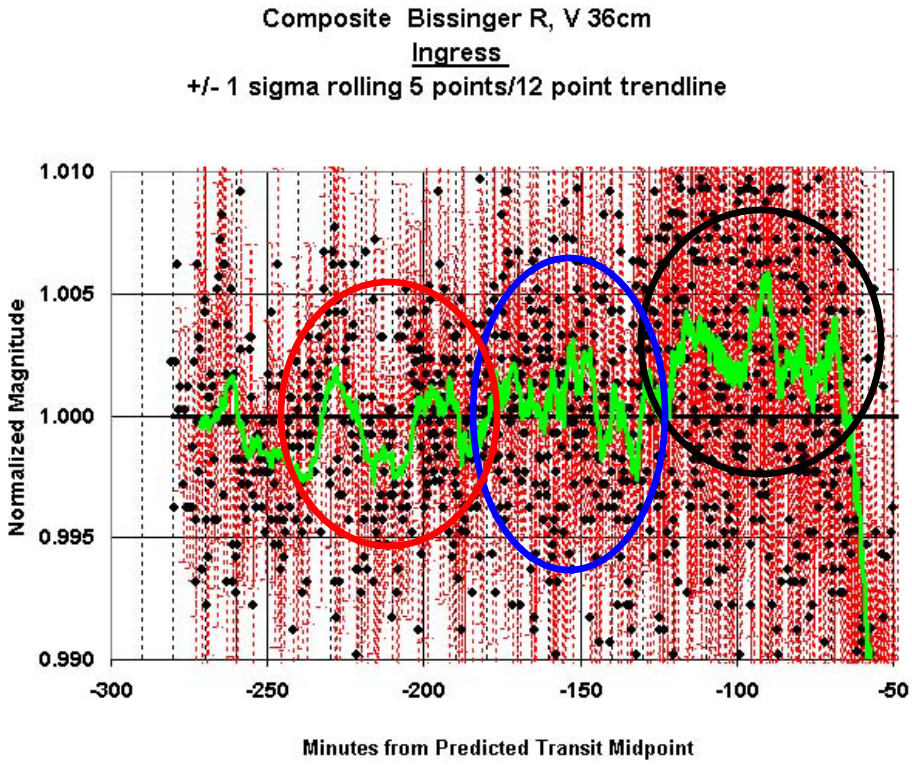

Figure 7 – Bissinger Ingress

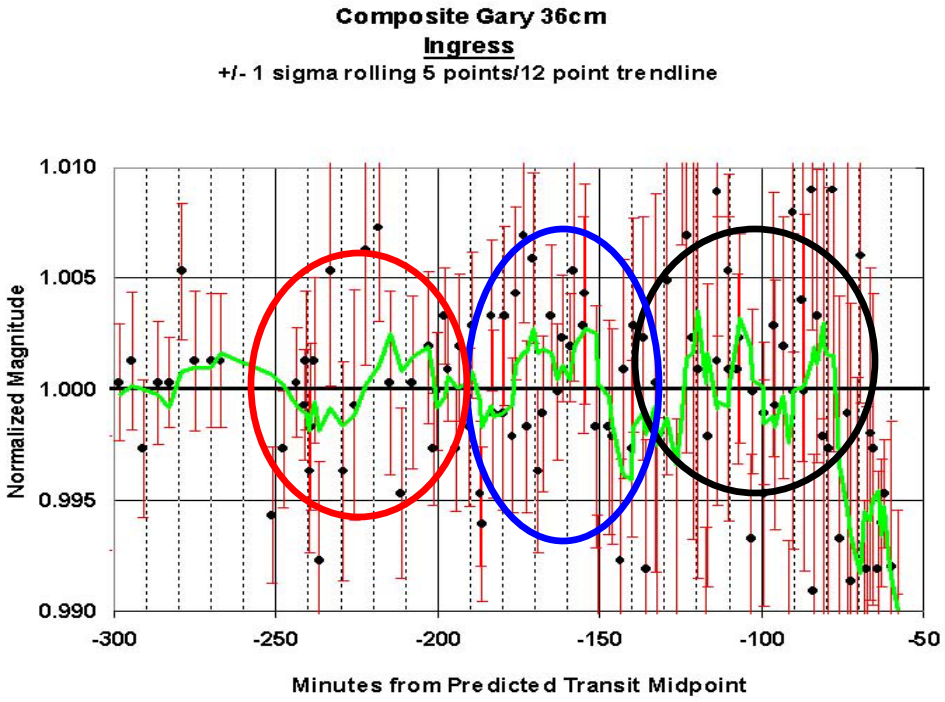

Figure 8 – Gary Ingress

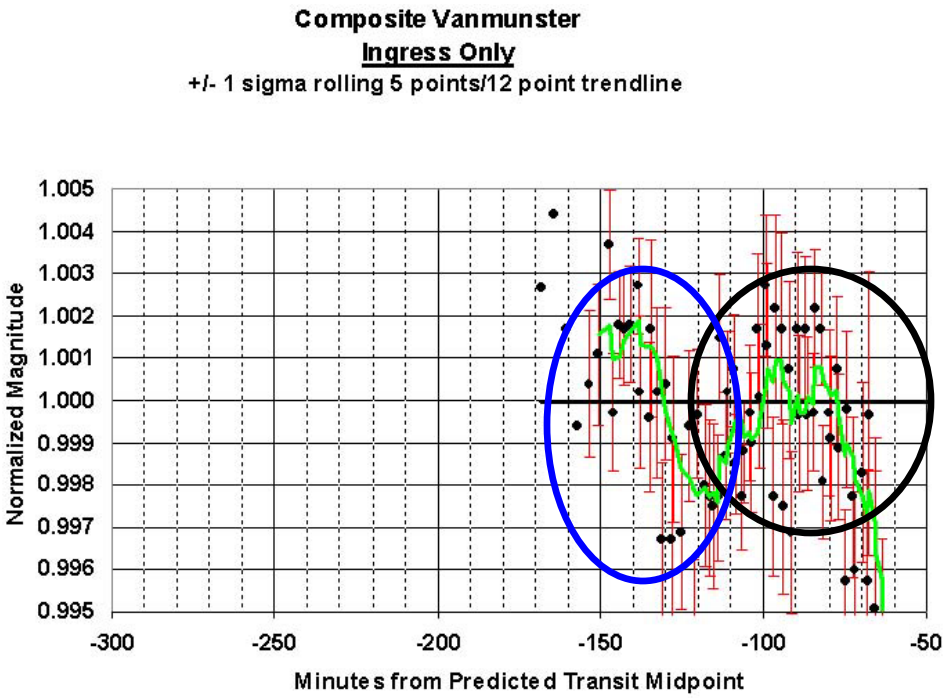

Figure 9 – Vanmunster Ingress

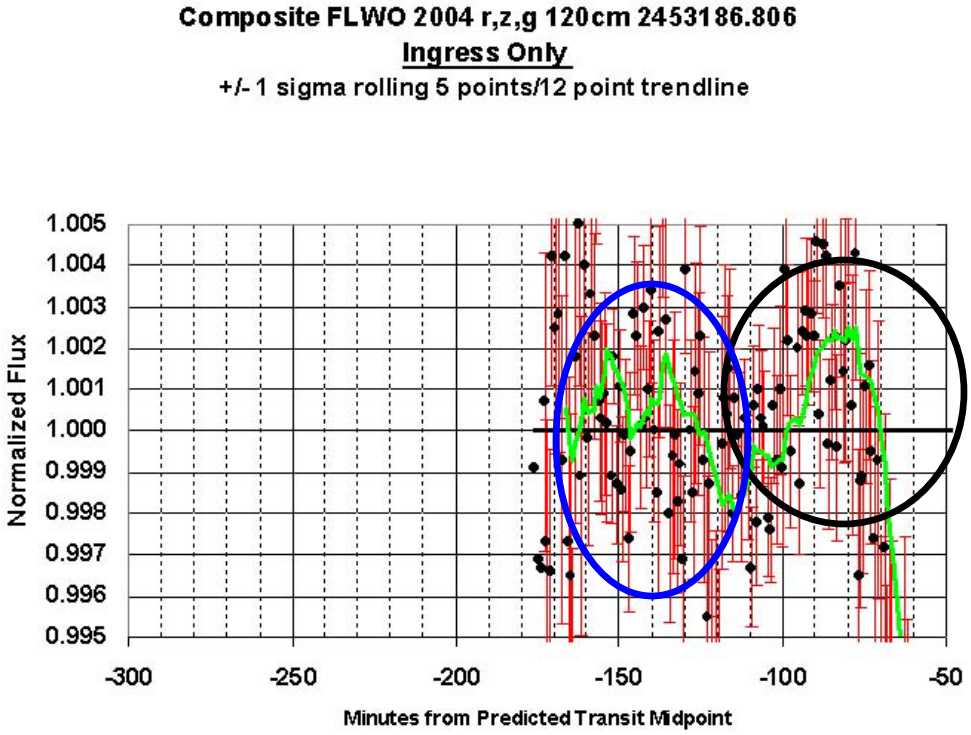

Figure 10 – FLWO Ingress

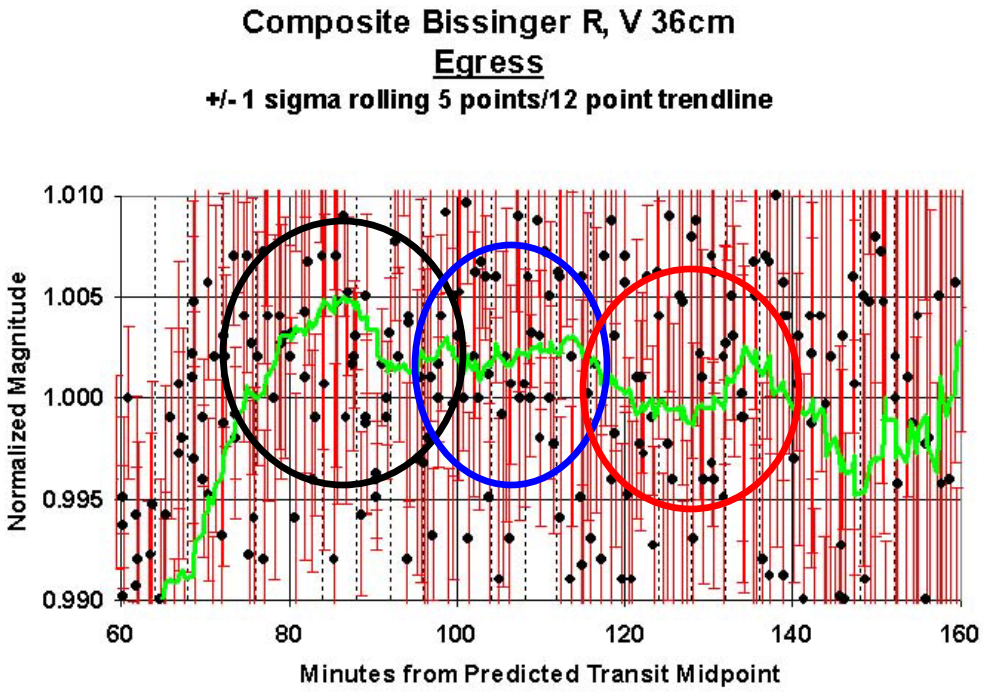

Figure 11 – Bissinger Egress

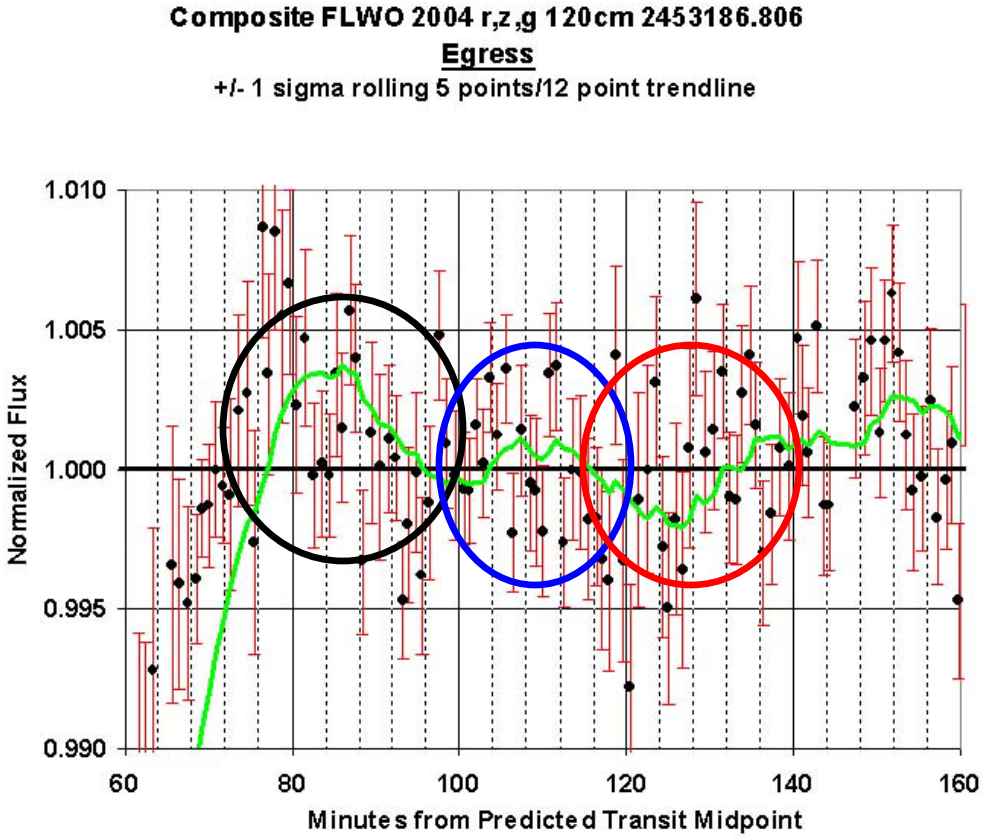

Figure 12 – FLWO Egress

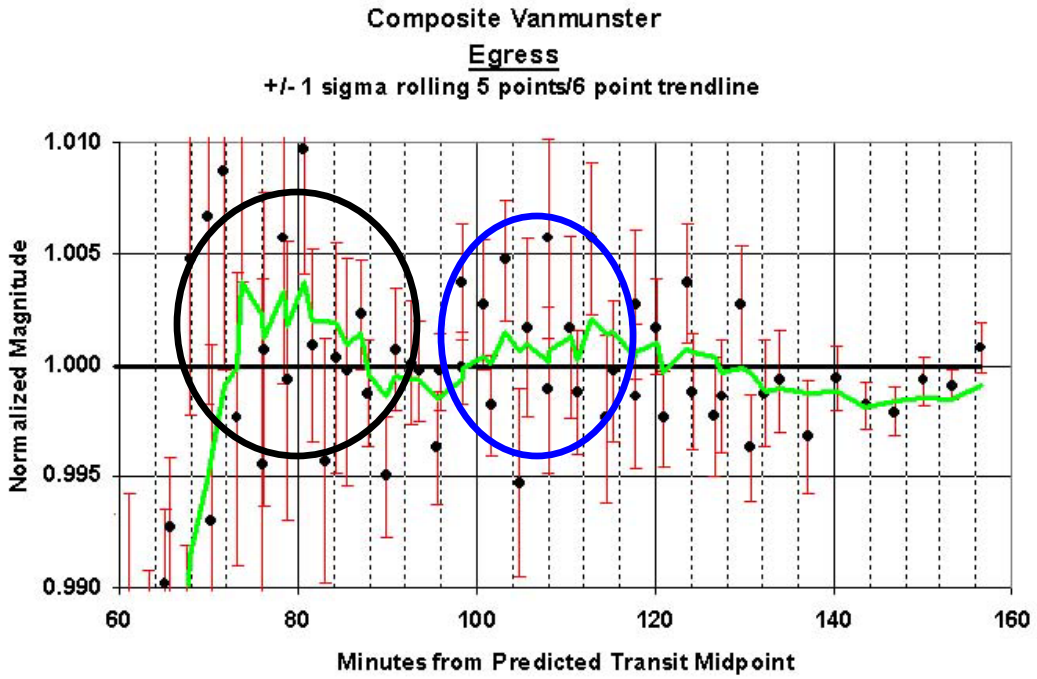

Figure 13 – Vanmunster Egress

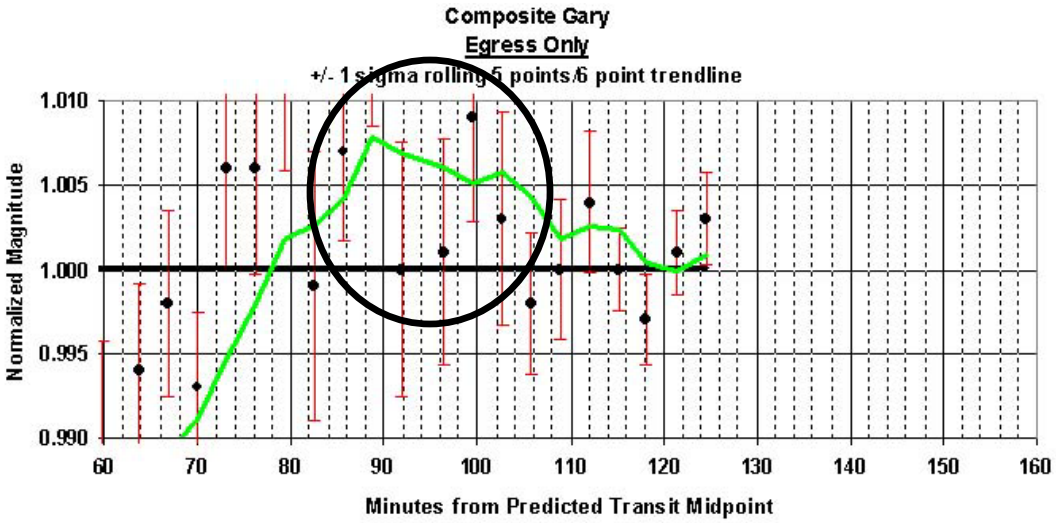

Figure 14 – Gary Egress

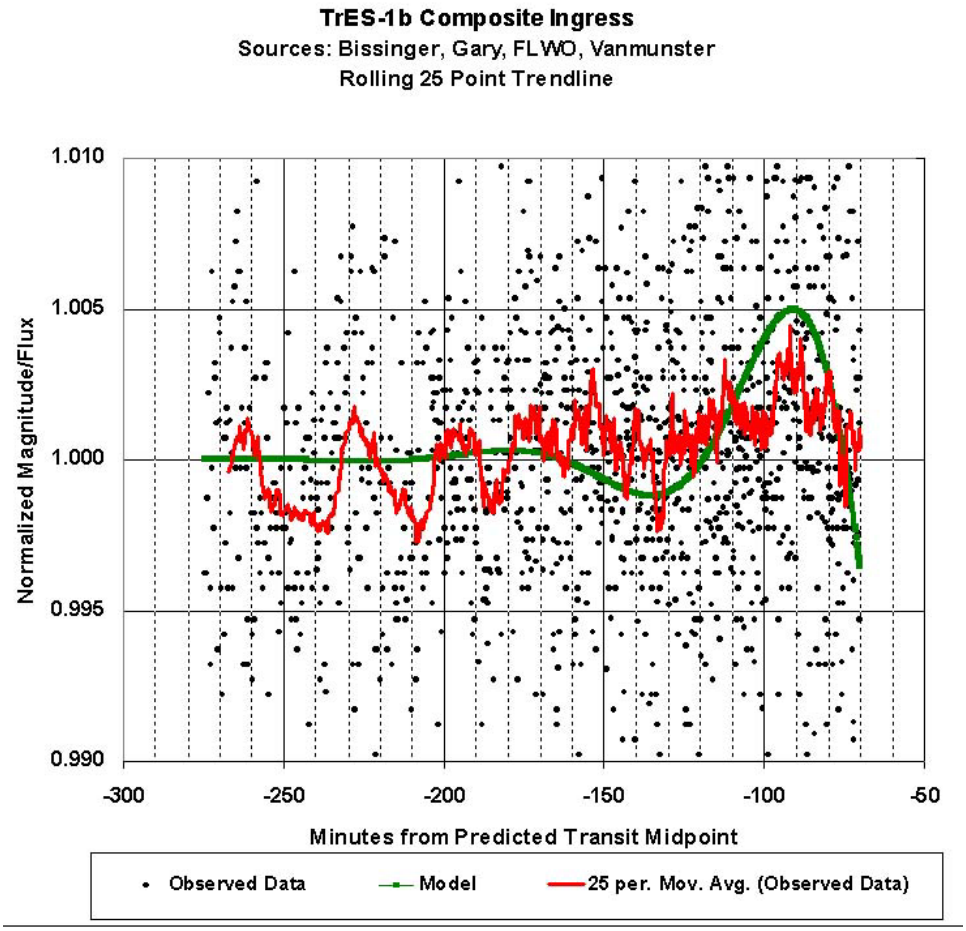

Figure 15 – Ingress Curvefit Model

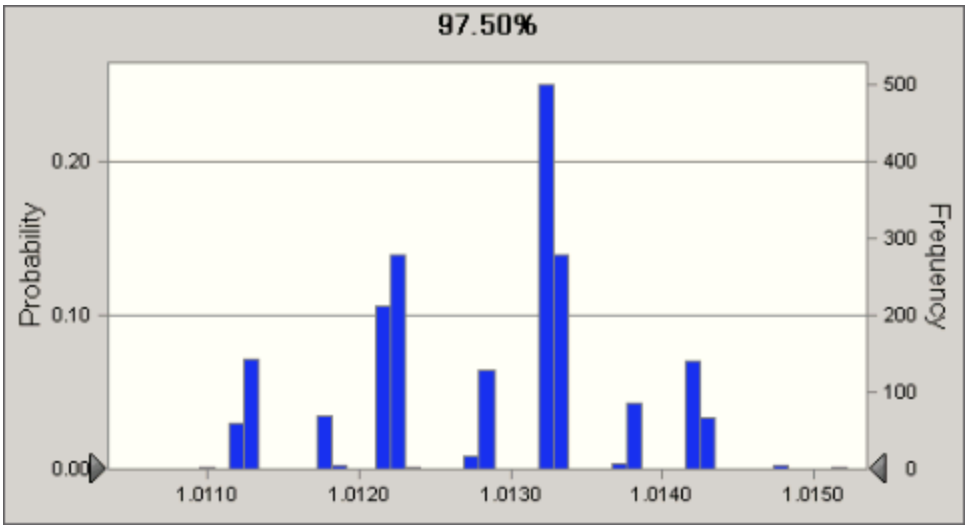

Figure 16 – 97.5% Confidence level of Mean for Bissinger Ingress Data

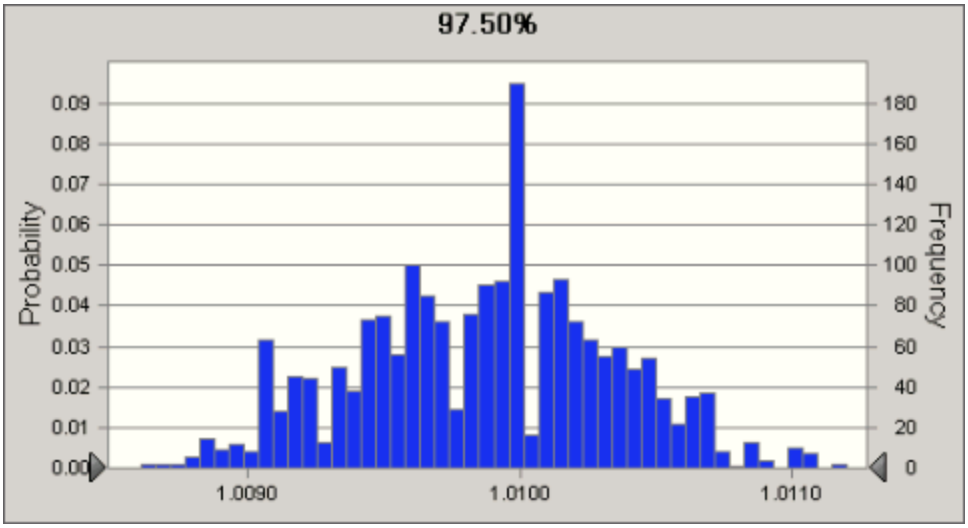

Figure 17 – 97.5% Confidence level of Mean for Bissinger Ingress Data after Model Application